Suppression of auto-resonant stimulated Brillouin scattering in supersonic flowing plasmas by different forms of incident lasers*

S S Ban(班帅帅)[1], Q Wang(王清)[1], Z J Liu(刘占军)[2], C Y Zheng(郑春阳)[2,†], and X T He(贺贤土)[1,2,‡]

[1] *HEDPS, Center for Applied Physics and Technology, School of Physics, Peking University, Beijing* 100871, *China*
[2] *Institute of Applied Physics and Computational Mathematics, Beijing* 100094, *China*

(Received 7 June 2020; accepted manuscript online 10 June 2020)

In supersonic flowing plasmas, the auto-resonant behavior of ion acoustic waves driven by stimulated Brillouin backscattering is self-consistently investigated. A nature of absolute instability appears in the evolution of the stimulated Brillouin backscattering. By adopting certain form of incident lights combined by two perpendicular linear polarization lasers or polarization rotation lasers, the absolute instability is suppressed significantly. The suppression of auto-resonant stimulated Brillouin scattering is verified with the fully kinetic Vlasov code.

Keywords: inertial confinement fusion, laser plasma interaction, stimulated Brillouin scattering, fully kinetic simulation

PACS: 52.38.–r, 52.65.–y **DOI:** 10.1088/1674-1056/ab9c12

1. Introduction

In both direct or indirect inertial confinement, stimulated Brillouin scattering (SBS) is one of the basic problem.[1–3] In a homogenous plasma, the absolute growth is easy to be stimulated when the matching condition of three-wave interaction is satisfied. However, in an inhomogeneous plasma the interaction area of SBS is restricted in a small resonant region because the matching conditions can be hardly satisfied.[4–6]

Recently, another mechanism in inhamogeneous plasmas, called autoresonance, is investigated, which will stimulate a significant spatial-independent growth of ion acoustic waves (IAWs). The autoresonant occurs because the nonlinear frequency shift compensates the detuning caused by the flow gradient and the SBS remain resonant automatically.[7,8] The autoresonat behavior of IAWs driven by the SBS process in supersonic flowing plasmas is performed by using the fully kinetic Vlasov code.[9] In those work, the flow velocity decreasing in the forward direction is defined as the "negative flow gradient", and the flow velocity increasing in the forward direction is defined as the "positive flow gradient". In the simulations, the stimulated Brillouin backscattering (SBBS) reflectivity in both positive and negative flow gradients reach the level of absolute growth which will scatter the incident light greatly.

In order to suppress the SBS in ICF, several methods have been applied. There are two mechanisms mainly proposed up to date. One is to optimize the uniformity of the incident laser spot such as spatial smoothing, spectral dispersion[10] and polarization smoothing,[11,12] the other is to decrease the interaction length of SBS such as the spike trains of uneven duration and delay (STUD),[13] alternating-polarization light,[14] polarization rotation[15] and two perpendicular linear polarization.[16] In this article, polarization rotation and two perpendicular linear polarizations are performed to suppress the absolute growth of auto-resonant stimulated Brillouin scattering. To find the effect of them, several simulations are performed by the 1-D Vlasov code[17] and theories associated with them are deduced.

The rest of the article is organized as follows: Theories of autoresonance of SBS and two different incident lights are presented in Section 2. Simulations based on the fully kinetic Vlasov code are shown in Section 3. Section 4 provides the conclusions and discussions.

2. Theory

2.1. Autoresonance of SBBS

In inhomogeneous plasmas, the three-wave interaction equations involves a nonlinear kinetic frequency shift in the forms as follows:[8,18]

$$(\partial_t + v_{g0}\partial_x + \nu_0)a_0 = \frac{-\mathrm{i}}{4}\delta\hat{n}_e a_1, \tag{1}$$

$$(\partial_t + v_{g1}\partial_x + \nu_1)a_1 = \frac{-\mathrm{i}\omega_0}{4\omega_1}\delta\hat{n}_e{}^* a_0, \tag{2}$$

$$\left(\partial_t + v_{g2}\partial_x + \nu_2 + \mathrm{i}\Delta(x) - \mathrm{i}\eta\left|\frac{\delta n_e}{n_e}\right|^{1/2}\right)\delta\hat{n}_e = \mathrm{i}4\gamma_0{}^2 a_0 a_1{}^*, \tag{3}$$

where $a_0 = eA_0/m_e c^2$ and $a_1 = eA_1/m_e c^2$ are the normalized vector potentials of incident light and the backscattered light;

*Project supported by the National Natural Science Foundation of China (Grant Nos. 11875091 and 11975059) and the Science Challenge Project, China (Grant No. TZ2016005).

†Corresponding author. E-mail: zheng_chunyang@iapcm.ac.cn
‡Corresponding author. E-mail: xthe@iapcm.ac.cn

$v_{g0}=ck_0/\omega_0$, $v_{g1}=ck_1/\omega_0$, $v_{g2}=(C_s+V)/c$ are the normalized group velocities of the incident light, backscattered light and IAWs, respectively; $\nu_2=\gamma_{LD}/\omega_0$ is the damping rate of IAWs; $\delta\hat{n}_e=\delta n_e/n_c$ is the density amplitude of IAWs. $\Delta(x)=v_{ga}[k_0(x)-k_1(x)-k_a(x)]$ is the spatial detuning, and it can be simplified by Talor expansion at the resonant point $\Delta(x)=v_{g2}k'(x-x_r)+v_{g2}k''(x-x_r)=K'(x-x_r)+K''(x-x_r)$. Here x_r is the initial resonant point, K' is defined as $K'=v_{g2}k'$, K'' is defined as $K''=v_{g2}k''$; and $\eta|\frac{\delta n_e}{n_e}|^{1/2}$ is the nonlinear kinetic frequency shift.

It is given as follows:

$$\frac{\delta\omega_{nl}{}^{\rm kin}}{\omega_a}=-\eta\left|\frac{\delta n_e}{n_e}\right|^{1/2}, \tag{4}$$

$$\eta=\frac{1}{\sqrt{2\pi}}\left[\alpha_i\sqrt{\frac{ZT_e}{T_i}}(v^4-v^2)\,e^{-\frac{v^2}{2}}-\alpha_e\right]. \tag{5}$$

When the detuning terms $K'(x-x_r)$ equals the kinetic detuning $\eta|\hat{n_e}|$, the wave-wave equations can be rewritten as

$$(\partial_t+v_{g0}\partial_x+\nu_0)a_0=\frac{-i}{4}\delta\hat{n_e}a_1, \tag{6}$$

$$(\partial_t+v_{g1}\partial_x+\nu_1)a_1=\frac{-i\omega_0}{4\omega_1}\delta\hat{n_e}^*a_0, \tag{7}$$

$$(\partial_t+v_{g2}\partial_x+\nu_2+iK''(x-x_r))\delta\hat{n_e}=i4\gamma_0{}^2a_0a_1{}^*. \tag{8}$$

Then a temporally growth mode would exist when $\Delta=e^{-i\pi/4}2^{-3/2}(K'')^{1/2}(\frac{\gamma_0^2}{v_{g1}v_{g2}})^{-3/4}\ll 1$.[19] The convective instability of SBS would turn to the absolute instability. The growth rate can be calculated by $\gamma=2\gamma_0(\frac{(v_{g1}v_{g2})^{1/2}}{v_{g1}+v_{g2}})-(\frac{v_1v_{g2}+v_2v_{g1}}{v_{g1}+v_{g2}})$ when $2\gamma_0>(\frac{v_1}{v_{g1}}+\frac{v_2}{v_{g2}})(v_{g1}v_{g2})^{1/2}$.

2.2. Absolute instability in the autoresonance of SBS

In the resonant area, when the growth of SBS turns to the absolute growth, the growth rate can be calculated by $\gamma_0=\frac{\omega_{pi}v_{os}\sqrt{k_0}}{2\sqrt{2}\sqrt{\omega_0c_s}}$, which is the absolute growth rate of SBS in a homogeneous plasma while the density of plasma equals the electron density of initial resonant point; $v_{os}=\frac{ea_0}{m_ec}$ and ω_0 is the frequency of incident light. Then $\gamma=2\gamma_0(\frac{(v_{g1}v_{g2})^{1/2}}{v_{g1}+v_{g2}})-(\frac{v_1v_{g2}+v_2v_{g1}}{v_{g1}+v_{g2}})$ and the reflectivity of SBS can be calculated by $I_r=I_{seed}e^{\gamma_{sat}}$ with t_{sat} being the growth interval before the saturation. The absolute growth area is determined by the resonant length L_r.[9]

In order to suppress the absolute growth of SBS in an inhomogenous plasma, rotation polarization and two perpendicular linear polarization with different frequencies are performed. For rotation polarization, the incident light is combined by two circle polarization lasers with different frequencies. The linear polarization of the incident light is slowly rotating, and it can be expressed as[15]

$$\boldsymbol{A}_0=a_0\cos(\omega_0t)[\cos(\Omega t)\hat{y}+\sin(\Omega t)\hat{z}], \tag{9}$$

where Ω is the frequency difference of these two circle polarization incident lasers. The growth rate of SBS in one direction is $\gamma_{y,z}=\gamma\cos(\frac{\Omega}{2}t)$.

As for two perpendicular linear polarizations, the incident light is formed by two linear lasers with different frequencies and their polarizations are perpendicular. This is different from the rotation polarization. The polarization of the incident laser varies between linear and ellipse and can be described exactly in theory.

$$\boldsymbol{A}_0=\boldsymbol{A}_y+\boldsymbol{A}_z=\frac{a_0}{\sqrt{2}}e^{i(k_1x-\omega_1t)}\hat{y}+\frac{a_0}{\sqrt{2}}e^{i(k_2x-\omega_2t)}\hat{z}, \tag{10}$$

where $\boldsymbol{A}_y$, $\boldsymbol{A}_z$, ω_1, ω_2, k_1, and k_2 are the vector potential, frequency, wave vector of incident lights with the polarization in y and z directions. The frequency difference Ω is defined as $\Omega=\omega_1-\omega_2$. The growth rate of SBS in one direction is $\gamma_{y,z}=\gamma\cos(\frac{\Omega}{2}t)$, the same as rotation polarization, and the reflectivity of SBS can be calculated by the time average of $\gamma_{y,z}$ in the growth time t_{sat}

$$I_{R_\Omega}=I_{seed}e^{\gamma_y t_{sat}}, \tag{11}$$

$I_{\Omega=0}$ and I_{seed} are the intensity of backscattering light when $\Omega=0$ and the seed light, respectively.

The time average of $\gamma_{y,z}$ in the growth time t_{sat} can be calculated by

$$\bar{\gamma}_y=\gamma\int_0^{t_{sat}}\left|\cos\left(\frac{\Omega}{2}t\right)\right|. \tag{12}$$

It can be simplified by the zero point of the cosine function as follows:[16]

$$\frac{\bar{\gamma}_y}{\gamma}=\begin{cases}\dfrac{\sin\left(\frac{\Omega}{2}t_{sat}\right)}{\left(\frac{\Omega}{2}t_{sat}\right)}, & \dfrac{\Omega}{2}<\dfrac{\pi}{2}\dfrac{1}{t_{sat}},\\ \dfrac{4}{\pi}\dfrac{\frac{\pi}{2}t_{sat}}{\frac{\Omega}{2\pi}}-\dfrac{\sin\left(\frac{\Omega}{2}t_{sat}\right)}{\left(\frac{\Omega}{2}t_{sat}\right)}, & \dfrac{\pi}{2}\dfrac{1}{t_{sat}}\le\dfrac{\Omega}{2}<3\dfrac{\pi}{2}\dfrac{1}{t_{sat}},\\ \dfrac{8}{\pi}\dfrac{\frac{\pi}{2}t_{sat}}{\frac{\Omega}{2\pi}}-\dfrac{\sin\left(\frac{\Omega}{2}t_{sat}\right)}{\left(\frac{\Omega}{2}t_{sat}\right)}, & 3\dfrac{\pi}{2}\dfrac{1}{t_{sat}}\le\dfrac{\Omega}{2}<5\dfrac{\pi}{2}\dfrac{1}{t_{sat}},\\ \dfrac{12}{\pi}\dfrac{\frac{\pi}{2}t_{sat}}{\frac{\Omega}{2\pi}}-\dfrac{\sin\left(\frac{\Omega}{2}t_{sat}\right)}{\left(\frac{\Omega}{2}t_{sat}\right)}, & 5\dfrac{\pi}{2}\dfrac{1}{t_{sat}}\le\dfrac{\Omega}{2}<7\dfrac{\pi}{2}\dfrac{1}{t_{sat}},\\ \cdots\end{cases} \tag{13}$$

3. Simulation

Firstly, the autoresonance of SBS is performed by one-dimensional Vlasov simulations and the physical parameters are related to the shock ignition.[20] The simulation length

is $L = 600\lambda_0$, including the length of the physical domain $L_p = 400\lambda_0$ and two-collision-layer length $L_b = 100\lambda_0$ both at the left and right boundaries. In the simulations, a positive flow gradient is applied, linearly ranging with the function $V(x) = c_s(\frac{x}{L} - \frac{7}{4})$ from $-1.5C_s$ to $-0.5C_s$ in the physical domain. Thus, the magnitude of flow gradient scale length is $|L_V| = |c_s/(\partial V/\partial x)| = 400\lambda_0$. In the physical domain, the electron density is ranged with the specific expression $n_e(x) = 0.1n_c/(\frac{7}{4} - \frac{x}{L})$ from $0.0667n_c$ to $0.2n_c$, and the simulation conditions are shown in Fig. 1. V and n_e keep the plasma flux or mass conservation in the physical domain.

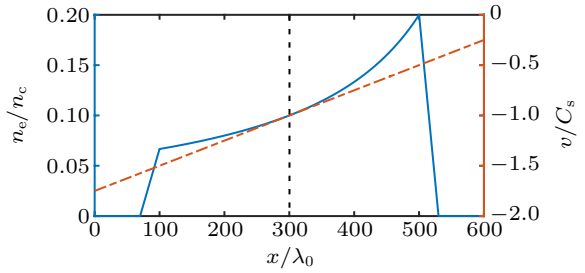

Fig. 1. Plasma flow profiles (orange-dashed lines) with the corresponding density profiles (blue-solid lines) of the positive flow gradient used in simulations.

In the simulations, the amplitude of incident laser is $a_0 = 0.015$ and the seed light is introduced from the right boundary with the same frequency as the incident laser, and its amplitude is set to be $a_1(x = L) = 0.01a_0$ to eliminate interference of the reflected light ($0.001a_0$) at the right boundary. The electron and ion temperatures are $T_e = 1.5$ keV and $T_i = 0.5$ keV. The ion charge and mass are $Z = 2$ and $m_i = 7344m_e$. Thus, $ZT_e/T_i = 6$, the negative kinetic nonlinear frequency shift due to ion trapping would be dominant. Here $x_r = 300\lambda_0$ is the initial resonant point where the plasma flow is $V(x_r) = -C_s = 1.15 \times 10^{-3}c$, plasma density is $n_e = 0.1n_c$ and $k\lambda_{De} = 0.33$.

At the initial resonant point, the frequency of IAWs in the homogeneous plasmas is $\omega_a = 2.1 \times 10^{-3}\omega_0$ and the growth rate of SBS is $\gamma_0/\omega_0 = 0.054a_0$. Then, the Rosenbluth gain of SBS in the presence of the normalized amplitude of the pump can be obtained by the first Talor expansion of spatial detuning K'

$$G_r = \frac{\gamma_0^2}{v_{g1}v_{g2}K'}. \tag{14}$$

For backscattering of SBS under the condition in the simulation, we have

$$K' = \left[\frac{1+M}{2M}\frac{\hat{n_e}}{1-\hat{n_e}} + 1\right]\frac{\omega_a}{v_{g2}L_v} \approx \frac{\omega_a}{v_{g2}L_v}. \tag{15}$$

Thus $G_{SBS} \approx \frac{\gamma_0^2 L_v}{v_{g1}\omega_a} = 2.34 \times 10^{-4}a_0{}^2$. On the other hand, the Rosenbluth gain of SRS can also be calculated by K'.

For backscattering of SRS,

$$K' = \frac{\omega_{pe}^2}{6k_0L_nv_e^2}\left(\frac{1}{2} - \frac{6v_e^2}{c^2}\right), \tag{16}$$

$$G_{SRS} \approx \left(\frac{v_{os}}{c}\right)^2 k_0L_n, \tag{17}$$

where L_n is the scale length of density gradient and it is defined as $L_n = n_e/(\partial n_e/\partial x)$. Because $\frac{G_{SRS}}{G_{SBS}} \approx 4\frac{(\omega_i)^2}{(\omega_{pi})^2} = 4\frac{m_i}{m_e}\frac{(\omega_i)^2}{(\omega_{pe})^2} \ll 1$, the growth of SRS in the expanding inhomogeneous plasma can be ignored.

In the simulations, with specific parameters $G_r = 5.27$ and $\gamma_0 = 8.1 \times 10^{-4}\omega_0$, the theoretical reflectivity of SBS can be predicted to be about 0.018, and the growth time of SBBS is about $2000T_0$.

The reflectivity variation of SBS is shown in Fig. 2. Obviously, the reflectivity of SBBS is consistent with the Rosenbluth gain at first but turn to be about 0.15 after about $15000T_0$. Another simulation under the same condition of the resonant point while $n_e = 0.1n_c$ in all the simulation box is performed, and it is shown in Fig. 3. Because of the existance of SRS, SBBS grows up after about $6000T_0$. The absolute growth reflectivity of SBBS in the homogeneous plasma is about 0.2. With the similar absolute growth processes, the wave-wave interaction in the resonant region in the inhomogeneous plasma when the growth turns to be the absolute growth can be deduced based on the equations in the homogeneous plasma.

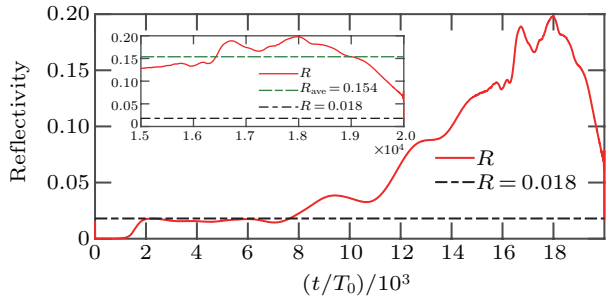

Fig. 2. Reflectivity of autoresonant SBS taken from the Vlasov simulations. The small graph shows the reflectivity and its average value when SBS saturates.

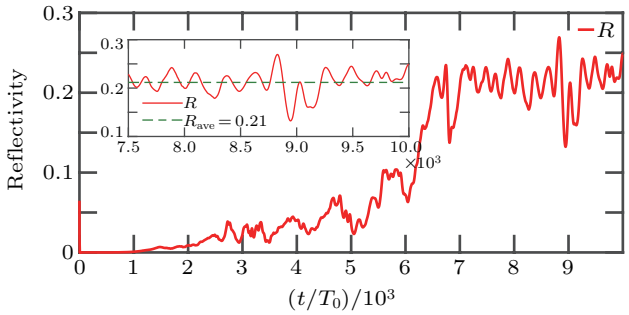

Fig. 3. Reflectivity of SBS in the homogeneous plasma when $n_e = 0.1n_c$.

In order to suppress the absolute growth of SBBS in the inhomogeneous plasma, rotation polarization and two perpendicular linear polarizations are performed. For the rotation polarization, two circular polarization lights are incident into the

plasma from perpendicular directions, marked as $\hat{y}$ and $\hat{z}$. The amplitude of the incident lasers are $a_0 = 0.015$. The seed light is at the frequency as the same as the incident laser, and its amplitude is set to be $a_1(x = L) = 0.01a_0$ as well. The frequency difference is chosen from $0.00002\omega_0$ to $0.002\omega_0$. Some results are shown in Fig. 4.

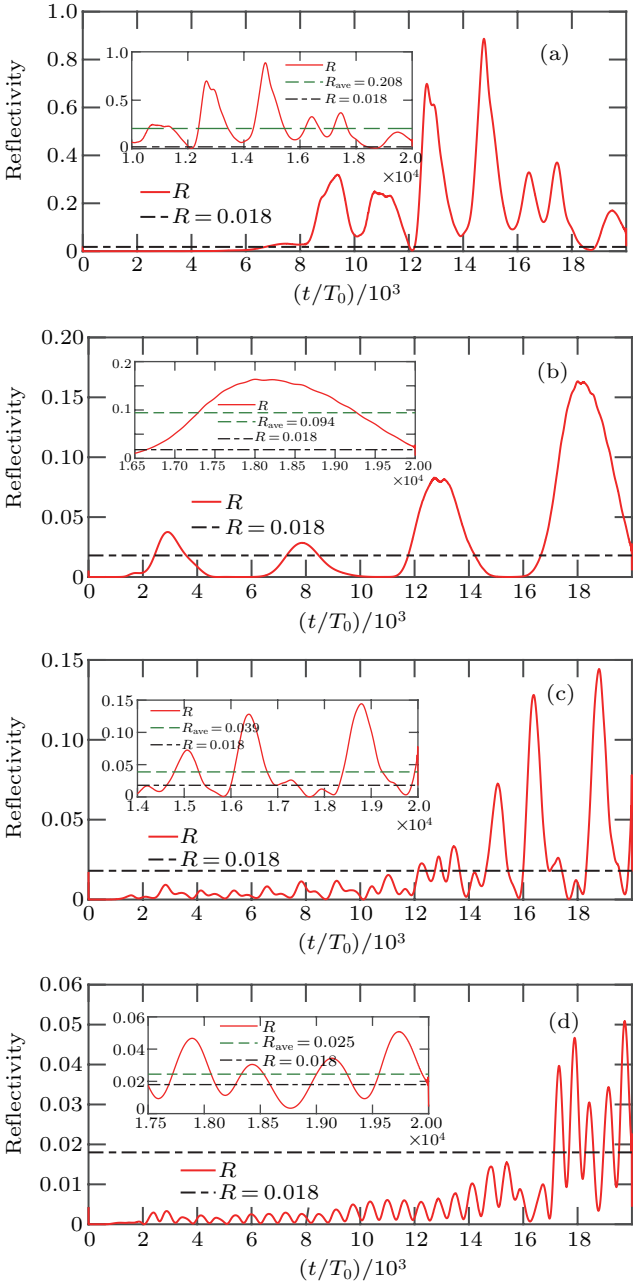

Fig. 4. Reflectivity versus polarization rotation frequency when $\Omega/\omega_0 = 0.00002, 0.0001, 0.0004, 0.0008$.

Physically, SBS would grow up when the polarization of incident light and backscattering light are in the same direction before the saturation. In $\hat{y}$ direction, for example, when the frequency difference is small, the polarization of the incident light almost does not change and it enhances the wave-wave interaction all the time till the saturation, thus the SBBS is not suppressed as the simulation shown in Fig. 4(a). With the increase of Ω, the polarization of the incident light varies from $\hat{y}$ direction to $\hat{z}$ direction in the growth interval, the growth rate of SBBS decreases for the reduction of the incident light in $\hat{y}$ direction and the reflectivity of SBS is suppressed to become smaller gradually. When the frequency difference is large enough, the polarization of the incident light would return back to $\hat{y}$ direction in the same growth interval, then it will enhance the interaction again. The reflectivity of SBBS will not be suppressed.

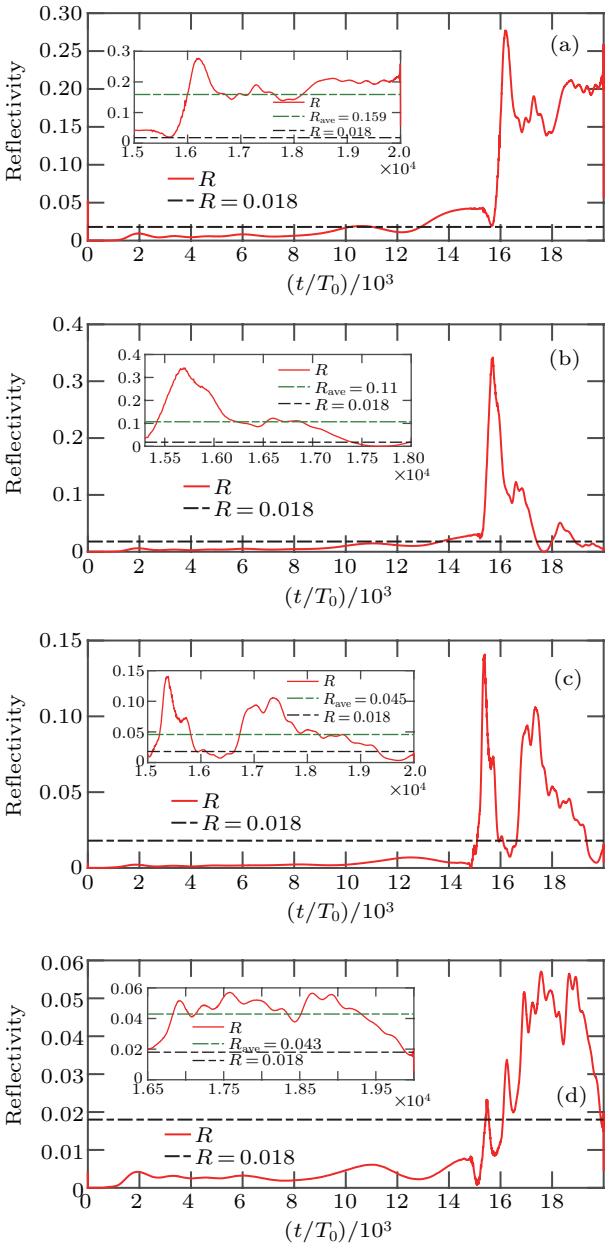

Fig. 5. Reflectivity versus the frequency difference by two perpendicular linear polarizations with different frequencies when $\Omega/\omega_0 = 0.0001$, 0.0002, 0.0004, 0.0013.

As for two perpendicular linear polarizations, the polarizations of these two perpendicular-linear-polarization incident lasers are in $\hat{y}$ and $\hat{z}$ directions as well. The amplitude of the incident lasers is $a_0/\sqrt{2} = 0.011$. The seed light is at the same frequency as the incident laser, and its amplitude is set to be $a_1(x = L) = 0.01a_0$. Frequency difference is chosen

from $0\omega_0$ to $0.002\omega_0$. Results of reflectivity from simulations of some frequency difference are shown in Fig. 5.

The physical mechanism of the two perpendicular linear polarizations is similar with the rotation polarization, but the polarization of the incident light varies between linear and ellipse instead of rotating around the x axis. Similarly, when Ω is small, most of the incident light is of linear polarization in y or z direction, and the SBBS will be enhanced till the saturation. When Ω becomes larger, SBBS will be suppressed because of the reduction of the incident light which matches the wave-wave equations. Saturation will appear when the Ω is large enough for several linear-ellipse cycles involved in the same growth interval.

The reflectivity versus the frequency difference is plotted in Fig. 6. By adopting both these two methods, the suppression of SBBS is significantly with the increase of frequency difference. The reflectivity decreases monotonically when Ω is small and reaches the saturation when $\Omega/\omega_0 = 10^{-3}$ in the condition of simulation parameters. The variation of reflectivity is consistent with the theory as it is showed in Fig. 6. And the minimum value of reflectivity appears when $\Omega/2$ is about $\frac{\pi}{2}\frac{1}{t_{\rm sat}} = 0.0004\omega_0$.

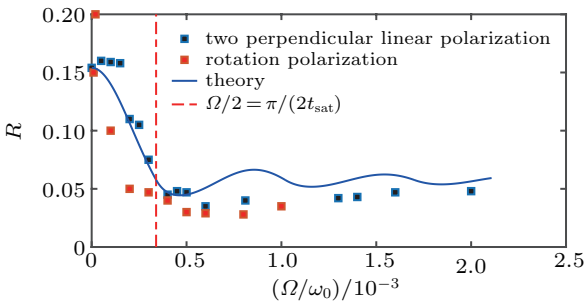

Fig. 6. Reflectivity versus the frequency difference for different forms of incident lasers.

Meanwhile, there are also some differences. The reflectivity by rotation polarization is suppressed faster and the minimum reflectivity is slightly smaller than the reflectivity of two perpendicular linear polarizations with different frequencies. In addition, for rotation polarization, the reflectivity of SBS has periodic oscillations because of the periodic oscillations of incident light. For two perpendicular linear polarizations with different frequencies, there is not any periodic oscillation in the reflectivity because of the constant amplitude of the incident light in y or z direction.

4. Conclusion

In summary, two different incident lights are performed to suppress the absolute instability caused by the auto-resonance of SBS. The suppression is obviously by adopting both methods with the increase of frequency difference. The reflectivity of SBBS decreases monotonically when Ω is small and reaches the saturation when $\Omega/\omega_0 = 10^{-3}$ under the condition of the simulation parameters with the increase of frequency difference. Considering that only two linear polarization lights are required by the method of two perpendicular linear polarizations, this method can be more conveniently used in experiment although the minimum of reflectivity by rotation polarization is slightly smaller.

Moreover, the reflectivity of convection growth of SBS is also suppressed in the simulations, it requires more further work to verify the suppression by different forms of incident lights.

Acknowledgement

We thank L. H. Cao for useful discussion.

References

[1] Hinkel D E, Rosen M D, Williams E A, Langdon A B, Still C H, Callahan D A, Moody J D, Michel P A, Town R P, London R A and Langer S H 2011 *Phys. Plasmas* **18** 056312
[2] Hinkel D E and Edwards M J 2013 *Plasma Phys. Control. Fusion* **55** 124015
[3] Craxton S, S Anderson K, Boehly T, N Goncharov V, Harding D, P Knauer J, Mccrory R, McKenty P, Meyerhofer D, F Myatt J, J Schmitt A, D Sethian J, W Short R, Skupsky S, Theobald W, L Kruer W, Tanaka K, Betti R, J B Collins T and Zuegel J 2015 *Phys. Plasmas* **22** 110501
[4] Drake J F, Kaw P K, Lee Y C, Schmid G, Liu C S and Rosenbluth M N 1974 *Phys. Fluids* **17** 778
[5] Rosenbluth M and Liu C 1972 *Phys. Rev. Lett.* **29** 701
[6] DuBois D, Forslund D and Williams E 1974 *Phys. Rev. Lett.* **33** 1013
[7] Maximov A, Oppitz R, Rozmus W and Tikhonchuk V 2000 *Phys. Plasmas* **7** 4227
[8] Williams E, Cohen B, Divol L, Dorr M, Hittinger J, Hinkel D, Langdon A, Kirkwood R, Froula D and Glenzer S 2004 *Phys. Plasmas* **11** 231
[9] Wang Q, Zheng C Y, Liu Z J, Cao L H, Xiao C Z, Feng Q S, Liu C S and He X T 2019 *Plasma Phys. Control. Fusion* **61** 085017
[10] Skupsky S, Short R W, Kessler T, Craxton R S, Letzring S and Soures J M 1989 *J. Appl. Phys.* **66** 3456
[11] Lefebvre E, Berger R L, Langdon A B, Macgowan B J, Rothenberg J E and Williams E A 1998 *Phys. Plasmas* **5** 2701
[12] Fuchs J, Labaune C, Depierreux S, Baldis H A and Michard A 2000 *Phys. Rev. Lett.* **84** 3089
[13] Afeyan B and Hller S 2013 *EPJ Web Conf.* **59** 05009
[14] Liu Z, Zheng C, Cao L, Li B, Xiang J and Hao L 2017 *Phys. Plasmas* **24** 032701
[15] Barth I and Fisch N J 2016 *Phys. Plasmas* **23** 102106
[16] Ban S, Wang Q, Liu Z, Zheng C and He X 2020 *AIP Adv.* **10** 025123
[17] Liu Z J, Zhu S p, Cao L H, Zheng C Y, He X T and Wang Y 2009 *Phys. Plasmas* **16** 112703
[18] Wang Q, Liu Z, Zheng C, Xiao C, Feng Q, Zhang H and He X 2018 *Phys. Plasmas* **25** 012708
[19] Liu C S, Rosenbluth M N and White R B 1974 *Phys. Fluids* **17** 1211
[20] Hao L, Li J, Liu W D, Yan R and Ren C 2016 *Phys. Plasmas* **23** 042702